

Galactic Evolution along the Hubble Sequence

Mercedes Mollá & Angeles I. Díaz

Departamento de Física Teórica, C-XI Universidad Autónoma de Madrid, Spain

September, 2002

Abstract.

A generalization of the multiphase chemical evolution model applied to a wide set of theoretical galaxies is shown. This set of models has been computed by using the so-called Universal Rotation Curve from (Persic, Salucci and Steel, 1996) to calculate the radial mass distributions of each theoretical galaxy. By assuming that the molecular cloud and star formation efficiencies depend on the morphological type of each galaxy, we construct a bi-parametric grid of models whose results are valid in principle for any spiral galaxy, of given maximum rotation velocity or total mass, and morphological type.

Keywords: galaxies: abundances, galaxies: evolution,galaxies:spirals

1. Introduction

There exist three important correlations (Vila-Costas and Edmunds, 1992; Oey and Kennicutt, 1993; Zaritsky, Kennicutt and Huchra, 1994; Dutil and Roy, 1999) among the observed characteristics of spiral and irregular galaxies: 1) The mass-metallicity relation: the more luminous the galaxy the higher its abundance; 2) The correlation between abundance and morphological type: earlier type galaxies have larger abundances than later type ones; and 3) The correlation between the radial gradient of abundances and the morphological type: The radial gradient of abundances is larger for later type galaxies than for earlier ones.

The problem appears when we see that the mass–metallicity relation seems to be the same for bright spirals and low-mass irregular galaxies while the correlation between the radial gradient and the morphological type has an effect on-off: when the galaxy mass decreases or the Hubble type changes to the latest irregulars, the steep radial gradient disappears and the abundance pattern becomes uniform for the whole disk.

To study correlations with a large number of galaxies for which we need a large number of models. For that, we build a bi-parametric grid of theoretical models depending on the galaxy total mass and morphological type.



© 2018 Kluwer Academic Publishers. Printed in the Netherlands.

2. Ingredients of the multiphase chemical evolution model

The scenario of the multiphase model begins with a spheroidal protogalaxy sliced into cylindrical regions. The gas of the protogalaxy has a mass $M(R)$ computed from the rotation curve $V(R)$, which we take from Persic, Salucci and Steel (1996) to calculate radial mass distributions $M(R)$ for any value of the luminosity.

This gas collapses onto the equatorial plane and forms out the disk. The infall rate is inversely proportional to a characteristic collapse time scale, which changes according to the total mass of the galaxy:

$$\frac{\tau_{col,gal}}{\tau_{col,MWG}} = \left[\frac{M_{MWG}}{M_{gal}} \right]^{1/2} \quad (1)$$

This implies that the characteristic collapse time scale $\tau_{col,gal}$ is longer for the less massive galaxies.

There exist different phases of matter in each radial cylinder: diffuse gas, molecular clouds, massive stars, low and intermediate mass stars, and remnants. The star formation in the halo follows a Schmidt law. In the disk the star formation has 2 steps: molecular clouds are formed from the diffuse gas. Then, stars form through cloud-cloud collisions, and from the interaction between massive stars and molecular clouds.

Every processes rates change along the galactocentric radius due to the volume of each region through a proportionality coefficient called efficiency or probability. Only the last described process does not change with R being constant for all galaxies. Moreover, the efficiency to form stars in the halo is assumed as constant for all halos. Thus, only efficiencies to form molecular clouds and to form stars from collisions among these ones, are variable for each galaxy.

The initial mass function was taken from Ferrini, Palla and Penco (1990) and the nucleosynthesis prescriptions are taken from Woosley and Weaver (1995) for $M > 8M_{\odot}$, Renzini and Voli (1981) for stars $0.8M_{\odot} < m < 8M_{\odot}$ and Iwamoto et al. (1999) for SN-I.

3. Model Results and Conclusion

We compute models for 44 radial mass distributions, and 10 different values of efficiencies between 0 and 1 which are equivalent to 10 morphological types, for each one. More details about models and results are described in Mollá, Díaz and Ferrini (2002).

These models reproduce the 3 cited correlations as we see in the following two figures. In Fig. 1 the radial distributions of the oxygen abundances, given by $12 + \log(O/H)$, are shown for 3 different rotation

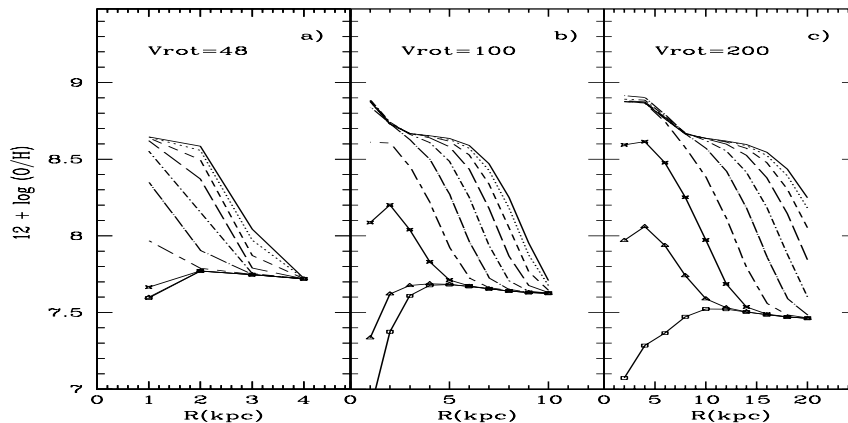


Figure 1. Radial of oxygen abundances for 3 different rotation velocities (in km.s^{-1}) as marked in each panel, by assuming ten different evolutionary rates or efficiencies for each one of them. These ten values represent ten morphological types, from $T = 1$, the top solid line, up $T = 10$, the bottom line with squares \square as symbols.

velocities as marked in panels. Ten different evolutionary rates or efficiencies, representing ten Hubble types, from $T = 1$, the top solid line, up $T = 10$, the bottom line with squares (\square) as symbols, are drawing for each one of them.

The more massive galaxies have strong abundance radial gradients only for the latest types ($T = 6 - 9$), except $T = 10$ which is flat, while the earliest ones have very flat radial distributions. The intermediate mass galaxies show steep radial distributions for the intermediate types ($T = 4 - 8$), the latest ones being rather flat. The less massive galaxies have no gradients for types later than 7, all the others showing very steep radial distributions. The described behavior is in agreement with the observed correlations. It is also clear from the same Fig. 1 that a minimum level of abundances is around 7.5 dex, which is the value found in the less enriched HII regions.

In Fig. 2, panel a) we represent the same oxygen abundances obtained with our 440 models for every radial regions as a function of the stellar magnitude of the same region, computed by assuming a ratio $M_*/L = 1$. These relation can not be exactly compared with data –panel b)– which represent characteristic oxygen abundances vs the magnitude of each galaxy, that is integrated quantities for a given galaxy, instead the local characteristics represented by the models. However, we can see that the correlation resulting from models have the same behavior than observations.

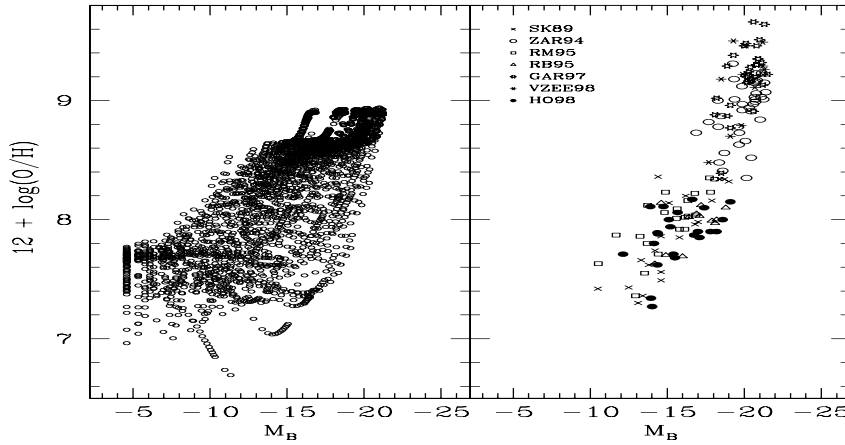


Figure 2. The mass-metallicity relation obtained for all radial regions of our 440 models. a) The oxygen abundance $12 + \log(O/H)$ vs the stellar luminosity in each region and model b) The data from Skillman, Kennicutt, and Hodge (1989)–SK89–, Zaritsky, Kennicutt and Huchra (1994)–ZAR94–, ? (?)–RM–, Roennback and Bergvall (1995)–RB95–, Garnett et al. (1997) –GAR97–, van Zee et al. (1998) –VZEE98– and Hidalgo-Gamez and Olofsson (1998) –HO98 as marked in the panel

Therefore, we conclude that our models follow adequately the observed trend for spiral and irregular galaxies.

References

- Dutil, I., and Roy, J.-R. 1999, ApJ, 516, 62
 Ferrini, F., Palla F., and Penco, U. 1990, A&A, 213, 3
 Garnett, D. R., Shields, G. A., Skillman, E. D., Sagan, S. P., & Dufour, R. J. 1997, ApJ, 489, 63
 Hidalgo-Gamez, A. M. & Olofsson, K. 1998, A&A, 334, 45
 Iwamoto, K., Brachwitz, F., Nomoto, K. et al. 1999, ApJSS, 125, 439
 Mollá, M., Díaz, A. I. and Ferrini, F. 2002, ApJ, submitted
 Oey, M. S., and Kennicutt, R. C. 1993, ApJ, 411, 137
 Persic, M., Salucci, P. and Steel, F. 1996, MNRAS, 281, 27, (PSS)
 Renzini, A., and Voli, M. 1981, A&A, 94, 175
 Richer, M. G. & McCall, M. L. 1995, ApJ, 445, 642
 Roennback, J. & Bergvall, N. 1995, A&A, 302, 353
 Skillman, E. D., Kennicutt, R. C., & Hodge, P. W. 1989, ApJ, 347, 875
 van Zee, L., Salzer, J. J., Haynes, M. P., O’Donoghue, A. A., & Balonek, T. J. 1998, AJ, 116, 2
 Vila-Costas, B., and Edmunds, M. G. 1992, MNRAS, 259, 121
 Woosley, S. E. and Weaver, T. A. 1995, ApJS, 101, 181
 Zaritsky, D., Kennicutt, R. C., and Huchra, J. P. 1994, ApJ, 420, 87